AD-778 380

TRANSACTIONS. TECHNICAL OPERATIONS OF THE MARITIME FLEET. THERMOCHEMICAL STUDIES. CONTROL OF CORROSION AND FOULING. CENTRAL SCIENTIFIC RESEARCH INSTITUTE OF THE MARITIME FLEET NUMBER 160, 1972

Naval Intelligence Support Center
Washington, D. C.

12 February 1974

DEPARTMENT OF THE NAVY
NAVAL INTELLIGENCE SUPPORT CENTER
TRANSLATION DIVISION
4301 SUITLAND ROAD
WASHINGTON, D.C. 20390

CLASSIFICATION: UNCLASSIFIED

APPROVED FOR PUBLIC RELEASE, DISTRIBUTION UNLIMITED

TITLE: Transactions. Technical Operations of the Maritime Fleet. Thermochemical Studies. Control of Corrosion and Fouling. Central Scientific Research Institute of the Maritime Fleet No. 160, 1972.
See Table of Contents.

AUTHOR(S): Various

PAGES: 61

SOURCE: Transactions. Technical Operations of the Maritime Fleet. Thermochemical Studies. Control of Corrosion and Fouling. Central Scientific Research Institute of the Maritime Fleet No. 160, 1972.
Pp. 17-26, 26-30, 30-38, 38-46, 68-72, 72-78, and 89-93.

ORIGINAL LANGUAGE: Russian

TRANSLATOR: LD

NISC TRANSLATION NO. 3514

APPROVED P.T.K.

DATE 12 February 1974

64

Transactions. Technical Operations of the Maritime Fleet. Thermochemical Studies. Control of Corrosion and Fouling. Central Scientific Research Institute of the Maritime Fleet No. 160, 1972.

Table of Contents

REDUCING THE CURE TIME OF THE LAST COAT OF ANTIFOULING PAINT

[Yu. Ye. Zobachev (Candidate of Technical Sciences) and S. T. Tsodikova. TRANSACTIONS. Technical Operations of the Maritime Fleet. Thermochemical Studies. Control of Corrosion and Fouling. Central Scientific Research Institute of the Maritime Fleet No. 160, 1972, pp. 17-26, Russian]

KhV-53 vinyl-base paint is now extensively used for protecting underwater hull areas against fouling. According to prevailing recommendations, the paint may be used over a fairly wide temperature range using the following cure periods (after applying the entire coating): 24 hours at temperatures above +15°C; 72 hours at 0 to +15°C; 120 hours -- from 0 to -10°C; 144 hours -- below -10°C.

The shortage of dock time sometimes compels the shipyard to violate these norms. According to foreign data [1], vinyl paint coatings do not require protracted curing prior to launching the ship. The Japanese firm "Tyupoku" suggests 2-3 days of ship dock time as adequate for painting the entire underwater hull area. There is no provision for additional cure time before launching the ship [2]. On the other hand, conditions for paint-and-varnish film formation affect considerably both the durability and protective properties of coatings [3,4].

The service properties of antifouling paints also depend on the drying conditions. Thus, the protective properties of incompletely dry vinyl paints may deteriorate [9] and cause cold running of the paint on a ship in motion [10].

The authors investigated the possibility of reducing the cure time of the antifouling paint KhV-53 (before launching) at various temperatures (including those in the winter).

The study included the physico-chemical characteristics, the duration of drying and reaching full hardness as a function of time and temperatures, the effects of different drying conditions on the antifouling properties of coatings, and the resistance of the coatings dried under various conditions to washout and cold running.

Along with the antifouling paint KhV-53, tests were also conducted on the regular anticorrosive ethynol-base

underwater hull paint EKZhS-40. The drying time for reaching full hardness was in this case rated according to OST (All-Union Standard) 10086-39 MI.17; the hardness was rated by GOST (State Standard) 5233-50.

The antifouling ability of the coating was determined by an accelerated glycine method [10]. The tests were conducted using the equipment of the Leningrad Branch of the State Research and Planning Institute and Leningrad Shipbuilding Institute. Films of antifouling paint were leached in glycine solutions (naCl, NaOH and amino acetic acid-glycine) for 3 days to approximate one year of operating a vessel in sea water.

The resistance of coatings to cold running was tested on a spindle machine [10] by rotating a painted disc (300-320mm in diameter) at 1050 rpm. A rough estimate of the friction resistance coefficient has shown that tests of coatings on discs are more rigid than on hulls of ships in actual operation.

The specimens were dried at 20, 10, 0, -5, and -10°C and were cured for 1, 2, 3, 4, and 5 days. The 10, 0, and -5°C temperatures were produced in a cooling chamber with 85-90% air humidity and limited air mobility. It was shown in study [11] that the drying time of a paint-and-varnish coating markedly increases with an increase in air humidity, beginning with 70%, and a decrease in air exchange rate. Thus, the conditions of film formation in the cooling chamber were more rigid than during painting in open air in the docks.

The time of reaching the state of full dryness of KhV-53 and EKZhS-40 paints is indicative of the solvent evaporation rate from the coating permitting determination of recoating time. Table 1 presents data indicating the full drying time of the tests paints.

After the solvent has evaporated from the paint, the film-forming processes continue for some time depending on the type of the binder. Converted polymers undergo chemical changes. The structural changes occurring in the unconverted polymers include shrinking of molecules to form supermolecular structural elements. In both cases, the entire set of physico-chemical properties of the coating also undergoes changes during this period. The hardness kinetics of the film is one of the typical indicators for the drying ability of the coating (Figures 1 and 2).

TABLE 1

Air temperature, °C	Paint drying time, hours							
	KhV-53				EKZhS-40			
	0.5	1.0	1.5	2.0	0.5	1.0	1.5	2.0
-10	Not dry	Not dry	Not dry	Dry	Not dry	Not dry	Not dry	Dry
- 5								
0								
10	Not dry	Dry	-	-	Not dry	Dry	-	-
20	Dry	-	-	-	Dry	-	-	-

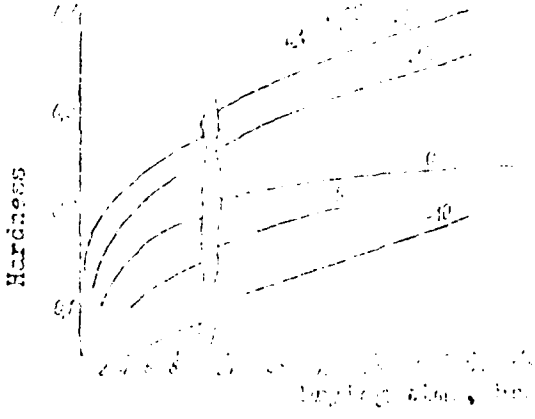

Figure 1. Effect of drying duration and temperature on the hardness of EKZhS-40 paint coats.

Figure 2. Changes in the hardness of a KhV-53 paint film as a function of temperature and drying time.

The hardness of the KhV-53 paint layer at -10, -5, and 0°C is very low (0.1-0.2) and remains constant for 18 days. The hardness of the EKZhS-40 layer at the same temperatures after 7 days is also low (0.2-0.3). At above-zero temperatures the hardness of the EKZhS-40 paint increases at a greater rate than that of the KhV-53 paint. After 7 days at +20°C the ethynol-base paint reaches a high hardness value of 0.7. Such high hardness values are typical of converted coatings. Ethynol lacquer is capable of converting by oxidative polymerization (using air oxygen) to an irreversible state even within 6-7 days [12]. The physical and mechanical tests conducted here have thus demonstrated that protracted curing of coatings on underwater hull portions in open air does not contribute to improving the service properties particularly at below-zero temperatures so that the assumed extended cure periods are by no means justified.

Further tests involving the effect of various drying conditions on the antifouling properties of the KhV-53 paint have demonstrated also the absence of deterioration of its protective properties. As may be seen from Table 2, the leaching rate of the toxines (couprous oxide) remains constant at all below-zero temperatures and is about 3.0 mg/cm^2.72 hours. The control specimens that were dried at room temperatures within 24 hours exhibited a leaching rate of 3.0 mg/cm^2.72 hours.

TABLE 2

Cure time in open air, days	Leaching rate, mg/cm^2.72 hours at various temperatures, °C		
	-10	-5	0
1	3.02	3.36	2.2
2	2.97	2.92	2.21
3	2.79	3.08	2.96
4	2.98	-	-
5	2.99	3.08	2.99

The test data on resistance of the coatings to cold running obtained on spindle machines are given in Table 3. To reduce the painting cycle, the discs were given a fewer number of coats -- three of EKZhS-40 paint and one of KhV-53. In this case the antifouling paint was applied to one-half of a disc. The drying time was evaluated from the half disc coated with the antifouling paint. The data in Table 3 provides drying times for the chart as a whole including the cure time of the last coat of the antifouling paint KhV-53.

It appears that the resistance of the paint to creeping depends not only on the curing of the last coat of the antifouling paint but also on the last coat of the anticorrosive paint. For example, there was hardly any cold running at -10°C by drying the last coats of EKZhS-40 and KhV-53 paints for 24 hours (specimen No. 13). A decrease in the drying time of the last coats of EKZhS-40 and KhV-53 to 15 hours impaired the coating quality (specimens Nos. 14 and 15). In this case creep was observed in the experimental speed range of 7-9 m/sec (about 14-18 knots). Similar regularities have been observed at other temperatures as well.

The tests results have shown a difference in the behavior of EKZhS-40 paint when recoated with antifouling paint and without it. On the chart with antifouling paint creep was observed to a lesser degree or was nonexistent at all. Cold running is still evident on specimens coated with an ethynol-base paint without a top coat of KhV-53 paint even after curing it for 5-6 days (specimens No. 7, 12, 16).

It could be assumed that the difference in the behavior of the coatings is due to the use of different type of binders and the nature of changes occurring in the coatings during film formation.

Table 4 presents the optimum drying conditions which were selected on the basis of the entire test set. The Table also provides drying conditions recommended by Ship Painting Regulations established by the Ministry of the Maritime Fleet (Departmental Specifications MVN-51.67).

The table indicates that protracted curing of the last antifouling paint coat prior to launching could be eliminated at all temperatures cited.

By and large the new painting schedules for the

TABLE 3

Number of Specimen	Temperature and humidity of air during drying	Coating chart and drying time of each layer in one-half of specimen	Test results in one-half of specimen	Coating chart and drying time of each layer on the second half of the specimen	Tests results on the second half of the specimen
1	18-20°C	EKZhS-40-4 EKZhS-40-4 EKZhS-40-8 KhV-53-8	No changes	EKZhS-40-4 EKZhS-40-4 EKZhS-40-16	No changes
2	18-20°C	EKZhS-20-2 EKZhS-40-2 EKZhS-40-2 KhV-53-4	No changes	EKZhS-40-2 EKZhS-40-2 EKZhS-40-6	Creep in the form of barely visible folds on 10-15% of the surface in the experimental speed range of 9.5-10.5 m/sec
3	10°C, 90%	EKZhS-40-4 EKZhS-40-4 EKZhS-40-4 KhV-53-4	No changes	EKZhS-40-4 EKZhS-40-4 EKZhS-40-8	Wrinkling with breaks down to the lower coat on 15-20% of the surface in the speed range of 10.5-11.6 m/sec
4	o°C, 90%	EKZhS-40-4 EKZhS-40-4 EKZhS-40-24 KhV-53-15	No changes	EKZhS-40-4 EKZhS-40-4 EKZhS-40-39	Creep in the form of folds on 5-7% of the surface in the experimental speed ranges of 8.5-9.5 m/sec

5	0°C, 90%	EKZhS-40-4 EKZhS-40-4 EKZhS-40-15 KhV-53-24	No changes	EKZhS-40-4 EKZhS-40-4 EKZhS-40-39	Creep with breaks down to the underlying coat on 30-40% of the surface in the experimental speed range of 7.0-8.4 m/sec
6	0°C, 90%	EKZhS-40-4 EKZhS-40-4 EKZhS-40-15 KhV-53-15	Creep on 15-20% of the surface in the experimental speed range of 8.5-9.5 m/sec	EKZhS-40-4 EKZhS-40-4 EKZhS-40-30	Creep with breaks down to the underlying coat on 40-50% of the surface in the experimental speed range of 5.2 m/sec
7	0°C, 90%	-	-	EKZhS-40-4 EKZhS-40-4 EKZhS-40-5	Creep in fine folds on 15-29% of the surface in the experimental speed range of 8.4-9.5 m/sec
8	-5°C, 90%	EKZhS-40-15 EKZhS-40-8 EKZhS-40-24 KhV-53-15	No changes	EKZhS-40-15 EKZhS-40-8 EKZhS-40-39	Slight wrinkling on 25% of the surface in the experimental speed range of 9.5-10.5 m/sec

	9	-5°C, 90%	EKZhS-40-15 EKZhS-40-8 EKZhS-40-15 KhV-53-24	No changes	EKZhS-40-15 EKZhS-40-8 EKZhS-40-39	Slight wrinkling on 25% of the surface in the experimental speed range of 10.5 m/sec
	10	-5°C, 90%	EKZhS-40-15 EKZhS-40-8 EKZhS-40-24 KhV-53-15	No changes	EKZhS-40-15 EKZhS-40-8 EKZhS-40-39	Slight wrinkling on 25% of the surface in the experimental speed range of 9.5-10.5 m/sec
	11	-5°C, 90%	EKZhS-40-8 EKZhS-40-15 EKZhS-40-12 KhV-53-12	Creep with breaks down to the underlying coat on 5-7% of the surface in the experimental speed range of 10.5 m/sec	EKZhS-40-8 EKZhS-40-15 EKZhS-40-24	Creep with breaks down to the underlying coat on 25% of the surface in the experimental speed range of 8.4-9.5 m/sec
	12	-5°C, 90%	-	-	EKZhS-40-8 EKZhS-40-15 EKZhS-40-5	Slight wrinkling on 10-15% of the surface in the experimental speed range of 9.5-10.5 m/sec

13	-10°C, 90%	EKZhS-40-15 EKZhS-40-8 EKZhS-40-24 KhV-53-24	No changes	EKZhS-40-15 EKZhS-40-8 EKZhS-40-25	Creep in fine folds on 30-40% of the surface in the experimental speed range of 9.5-10.5 m/sec
14	-10°C, 90%	EKZhS-40-15 EKZhS-40-8 EKZhS-40-15 KhV-53-24	Creep with breaks down to the underlying coat on 50-60% of the surface in the experimental speed range of 8.4-9.5 m/sec	EKZhS-40-15 EKZhS-40-8 EKZhS-40-37	Creep with breaks down to the underlying coat over the entire surface
15	-10°C, 90%	EKZhS-40-15 EKZhS-40-8 EKZhS-40-24 KhV-53-15	Creep with breaks down to the underlying coat on 15-20% of the surface in the experimental speed range of 7-8.4 m/sec	EKZhS-40-15 EKZhS-40-8 EKZhS-40-8	Creep with disruption down to the underlying coat over the entire surface

16	-10°C, 90%	-	-	EKZhS-40-15 EKZhS-40-8 EKZhS-40-6	Creep with breaks down to the underlying coat on 15-50% of the surface in the accelerator speed range of 5.2-9.5 m/sec

TABLE 4

No. of layer	Paint name	Coating drying time, hours at temperatures °C				
		-10	-5	0	10	20
	A. According to test results					
1	EKZhS-40	8-15	8-15	4	4	2
2	EKZhS-40	8-15	8-15	4	4	2
3	EKZhS-40	8-15	8-15	4	4	2
4	EKZhS-40	24	15	15	4	2
5	KhV-53	4	4	4	4	4
6	KhV-53	24	24	24	4	4
	Total	76-97	67-38	55	24	16
	B. According to Ship Painting Regulations, Ministry of the Maritime Fleet					
1	EKZhS-40	8-15	8-15	6-8	4-6	2-4
2	EKZhS-40	8-15	8-15	6-8	4-6	2-4
3	EKZhS-40	8-15	8-15	6-8	4-6	2-4
4	EKZhS-40	24-36	24-36	16-24	8-16	4-8
5	KhV-53	4-10	4-10	4	4	4
6	KhV-53	4-10	4-10	4	4	4
Curing		120	120	72	72	24
	Total	176-221	176-221	114-128	100-114	42-52

KhV-53 paint would reduce ship dock time from 7-9 to 3-4 days at -10, -5°C; from 4-5 to 2 days at 0°C; from 4-2 days to 1.0-0.5 days at above-zero temperatures.

The new cure schedules for the KhV-53 paint are presently being checked under operating conditions on ships of the Baltic and Latiran shipping lines following which they will be included in the Ship Painting Regulations (of the Ministry of the Maritime Fleet).

REFERENCES

1. Catalogs of "Chugoku Toryo Co. Ltd."; "Jotun Surety System for Ships"; "Marine Painting Specifications and Product Data by International"; "Hempels Marine Paints".

2. Report on the Visit of a Soviet Specialist Delegation to Japan for Studying the Production Technology and Application of Paints for Hull Protection Against Corrosion and Fouling. Leningrad. TsNIIMF (Central Scientific Research Institute of the Maritime Fleet), 1970.

3. Zubov, P.I. and Golikov, V.S. Issledovaniye dolgovechnosti polimernykh pokrytiy v zavisimosti ot usloviya formirovaniya i stareniya. (Study of the Durability of Polymer Coatings as a Function of Film-Forming Conditions and Curing). DOKLADY AN SSSR (Transactions of the Academy of Science USSR), v. 161, No. 4, 1965.

4. Zubov, P.I., Sukhareva, L.A. and Golikova, U.S. Issledovaniye dolgovechuosti alkidnyich pokrytiy (Study of the Durability of Alkyd Coatings). Mekhanika Polimerov, No. 3, 1965.

5. Sukhareva, L.A. Golikova, V.S. and Zubov, P.I. Vliyaniye vodnoy sredy na vnutrenniye napryazheniya v alkidnykie pokrytiyakh (Effect of a Water Environment on Internal Stresses in Alkyd Coatings). Lakokrasochnyye Materialy i ikh Primeneniye, No. 1, 1965.

6. Kozlov, P.V. and Braginskiy, G.I. Khimiya i tekhnologiya polimernykh plenok (Chemistry and Technology of Polymer Coatings). Moscow, Khimiya, 1965.

7. Peyn, G.F. Tekhnologiya organichesnikh pokrytiy (Technology of Organic Coatings), v.1. Leningrad. Goskhimizdat Publishing House, 1959.

8. Drinberg, A.Ya., Gurevich, Ye S. and Tikhomirov, A.V. Tekhnologiya nemetallicheskikh pokrytiy (Technology of Nonmetallic Coatings), Leningrad Goskhimizdat Publishing House, 1957.

9. Ragg, M. Zashchita sudov ot obrastaniya i korrozii (Protection of Ships Against Corrosion and Fouling).

Leningrad, Sndpromgiz Publishing House, 1960.

10. Morskoye obrastaniye i bor'ba s nim (Marine Fouling and its Control). Moscow, Koyenizdat Publishing House, 1957.

11. El'terman, V.M. Ventilatsiya pri proizvodstve malyarnykh rabot. Ventilation for Painting Operations. Industrial Ventilation. LDNTP (Leningrad House of Scientific and Technical Propaganda), 1967.

12. Dolgopol'skiy, I.M. Adl. Lak etinol' (Ethynol Lacquer), Moscow. Goskhimizdat Publishing House, 1963.

PROCEDURE OF DETERMINING THE ADHESION OF THERMOPLASTIC COATINGS

[By G.I. Shcherbinina and Yv.M. Kaplin. In "Tekhnicheskaya ekspluatatsiya morskogo flota. Teplokhimicheskiye issledovaniya. Bor'ba s korroziyey i obrastaniyem" (Technical Operations of the Maritime Fleet. Thermochemical Studies. Control of Corrosion and Fouling). Transactions of the Central Scientific Research Institute of the Maritime Fleet. No. 160, 1972, "Transport" Publishing House, Leningrad; pp. 26-30, Russian]

In the development and use of paint-and-varnish coatings for protecting underwater ship areas against corrosion and fouling, one of the principal requirements imposed upon them is their high adhesion to both the metal and the primary layer. Good adhesion contributes to a longer service life of the paint-and-varnish coating and a reliable protection.

Studies [1, 2, 3] describe various procedures for both quantitative determinations of coating adhesion to metals of which most extensively used is the method of adhesion based on critical values [4]. The essence of this method lies in the fact that internal stresses increase linearly with the thickness of the coating being formed to a certain critical value at which spontaneous separation of the film from the substrate occurs. The phenomenon is related to stresses occurring during film formation at the film-substrate boundary; these stresses act against the forces of adhesion much like mechanical tensile stresses and, upon reaching the critical value, break the film-substrate bond. Thus, adhesion may be rated on the basis of critical stresses in the film.

The cantilever method was selected for determining stresses in thermoplastic coating [5] in which stresses, occurring in the film of an adequately strong bond, bend the substrate and force it free from its initial position. The stress value is determined from the following formula

$$\sigma = \frac{Eht}{3l\Delta t}, \text{ kg/cm}^2$$

where h is the value of cantilever deflection, c; E is the modulus of elasticity; t is the thickness of the substrate, cm; l is the length of the film, cm; Δt is the thickness of the coating, cm.

The stress tests substrates were made of heat-treated steel tape (GOST 2614-65) measuring 0.5 x 15 x 120 mm. The substrate's working area was 90 mm long.

Rosin- and paraffin-base compositions (GOST 797-41 and GOST 784-53, respectively) were used for preparing the coating material.

Prior to applying the coating, the substrates were cleaned with fine abrasives, degreased with an alcohol-ether mixture, and dried. The specimens were placed on a strictly horizontal surface and painted. The thermoplastic coating was applied from a melt heated to 110-120°C.

Figure 1 shows curves reflecting stresses of the thermoplastic coatings as a function of their thickness and rosin contents in them. The internal stresses were

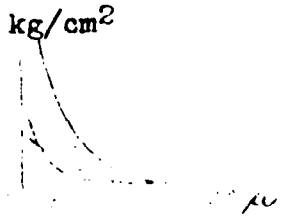

Figure 1. Changes in internal stresses as a function of film thickness:

1 -- rosin, 30%, paraffin, 20%; 2 -- rosin, 50%; paraffin, 50%; 3 -- rosin, 70%; paraffin 30%.

found to decrease with increasing film thickness and rosin content. The relationship between the film thickness and the stresses permits stress extrapolation at the film-substrate interface. Thus, for 30% of rosin in the paraffin and a film thickness of 25μ, the stress is about 40 kgf/cm^2 and when the rosin content is increased to 50%, the stress for the same film thickness drops down to 20 kgf/cm^2. It may be well to point out that the internal stress for a film thickness above 400μ is negligible.

The drop of stresses in the paraffin-rosin system with increasing the percentage of rosin may be attributed

to an increase in the content of functional COOH groups constituting the resionous acids of the rosin which contribute to strengthening the bond between the coating and the substrate. The adhesion of a film with a high rosin content to metal exceeds the internal stresses; as a result, the film stretches and cracks due to the composition's low cohesive strength.

A similar phenomenon was observed in films that were formed from a rosin solution in alcohol-ether mixture. Figure 2 shows the kinetics of changes in the internal stresses of a rosin film applied to a steel substrate.

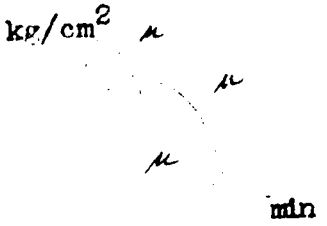

Figure 2. Kinetics of changes in internal stresses in a rosin film.

The process begins with the evaporation of the solvent and an increase in internal stresses with their subsequent decrease. Total solvent removal causes a drastic drop of stresses. The latter is caused (as indicated earlier) by the cracking of the coating. Hence, the internal stresses in a 100μ thick film consisting of 70% rosin and 30% paraffin reach their critical value at this point.

The data obtained here on thermoplastic coatings adhesion to metal correlate well with those obtained by the uniform break-away method. The principle of this method lies in the fact that the magnitude of adhesion is rated by the force required to separate the adhesive from the substrate. In this case the force is applied perpendicularly to the coating surface. A 4s-steel die (35 mm in dia.) with a flat working end was used to determine the adhesion of thermoplastic coatings. Dies with grooved end surfaces were used as needed.

For applying the thermoplastic coating, the die was heated in a thermostatically controlled chamber to 10°C below the minimum coating application temperature and

then pressed into the coating. The die depression depth was controlled by three stops (depending on purpose) set on the threaded surface of the die. The stop positions were determined by a micrometric depth gage.

The break-away of the test coatings was characterized by one of three modes of failure:

-- adhesive, where the coating peeled off completely from the surface;
-- cohesive, in which the coating in itself was broken;
-- combined, where both the adhesive and cohesive failures occurred.

Prior to use, the die was thoroughly cleaned, degreased and dried. The coatings were applied at 110-120°C and cooled at room temperatures. The tests were conducted on a tensile-testing machine.

Figure 3 shows a directly proportional curve film-substrate bond strength versus rosin content in the coating. As the percentage of the rosin in the paraffin-rosin system is increased, the value of adhesion rises. The resinous acid molecules in the rosin form a strong bond through the polar COOH groups, so that the greater the number of polar groups in the boundary layer, the stronger the bond.

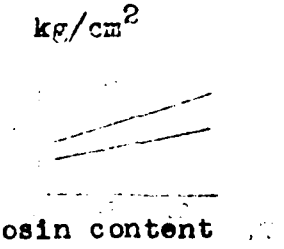

Figure 3. Film-substrate bond strength as a function of rosin contents.

As the film thickness is increased (Figure 4), the internal stresses, which had occurred in the adhesive during film formation, reduce the forces of interaction between the film and the substrate and weaken the adhesive strength.

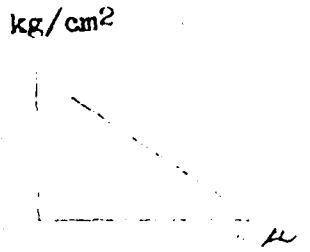

Figure 4. Film-substrate bond strength as a function of thickness of a film containing 80% rosin and 20% paraffin.

The testing of the adhesive strength of rosin-and-paraffin-base thermoplastic materials destroys the bulk phase which is the weakest link in compositions of this type. Unlike the boundary layer where the molecular arrangement is strictly oriented [6], it is chaotic in the bulk phase which reduces the forces of interaction between the molecules and the composition's cohesive strength related to them.

During the formation of the bond between the film and the substrate in rosin-paraffin-base compositions, the deformation in the bulk phase develops to a value corresponding to that of teh mechanical strength of the composition. The low mechanical strength of the latter and the adhesion to the metal exceeding this strength cause the internal stresses to drop due to the cracking of the coating.

The inadequate mechanical strength of rosin-base films is due to the inhomogeneity of the rosin.

Conclusion

1. A feasibility study has been made to determine the adhesive strength of thermoplastic coatings by the method of critical values and the uniform break-away technique.

2. The adhesive strength of thermoplastic coatings is a function of rosin content and film thickness.

3. With an increase in rosin content, the internal stresses drop while the film-substrate bond strength increases.

OPERATING TESTS OF THE CATHODIC PROTECTION SYSTEM "LUGA" ON THE MOTOR SHIP KAPITAN PLAUSHEVSKIY

[Kysotskiy, A.A.; Central Scientific Research Institute of the Maritime Fleet, TRANSACTIONS, Technical Operations of the Maritime Fleet. Thermochemical Studies. Corrosion and Fouling Control, No. 160; Leningrad "Transport" Publishing House, 1972, pp. 30-38, Russian]

Hull corrosion of seagoing vessels is related not only to metal properties but also to the sea water salinity and temperature (salinity determining the electric conductivity of sea water and, hence, metal corrosion rates).

On ships sailing in low-salinity basins the corrosion processes are inhibited and are concentrated at the boundaries of the cathodic and anodic areas causing pitting -- the most dangerous type of corrosion. Sea water temperature not only governs changes in the electrochemical potentials of metals and the electrical resistance of the water but also promotes corrosion processes. In the tests conducted under actual operating conditions involving controlled current densities and hull potentials -- as cathodic protection efficiency indices, primary consideration was given to the effects of sea water temperature and salinity on electrochemical protection parameters (particularly on potential distribution over the hull and protective current density). The operating tests were conducted on the motor ship KAPITAN PLAUSHEVSKIY whose underwater hull area was painted four months earlier on the basis of a standard chart.

The measurements of the potential distribution over the hull were done at anchor in ports and in roadsteds as well as during special stops (in the Arabian Sea on 11 January 1971 prior to reaching the port of Bombay; also on 21 March 1971 in the Mozambique Strait on the cruise from Colombo to Odessa).

The measurements were done in the area of frames 0, 10, 23, 45, 54, 70, 84, 100, 113, 130, 143, 155, and 170. The portable reference electrode was used 7-9m below the waterline depending on the draft; the potentials were measured every other meter. Noteworthy is the fact that the potential distribution over the hull was fairly uniform except for one case when the ship was in fresh water; in this case the potential variations in the anode areas were rather distinct from one frame to the other. The cylindrical area of the outer hull plating exhibited

potential variations of 50-100mv; in the anode area of the bilge the potential was 2 to 2.5 times that of the protective level (Figure 1).

Numerous measurements taken during the cruise both at anchor and underway showed potential drop rates to its initial value (650-750mv) and its rises to the protective level (850mv). The findings cited in Figure 2 were obtained in the Atlantic Ocean during the cruise from Las Palmas to Cape Town at average speeds of 14.5 knots.

Curve 1 shows the protective effect of salt deposits in the pores of the paint coats after current cutoff. These deposits close up the pores and restrict oxidizer supply to the metal's surface thus inhibiting hull potential displacement toward the positive. Curve 2 indicates a potential rise to 850mv for a steady-state current density of 0.0041 a/m^2 (prior to disconnection) which takes 7 hours. With a current density of 0.032 a/m^2 (Curve 3) the protective potential level is achieved within 20 minutes. The curves that were plotted on the basis of data obtained on the ship at anchor are similar to those in Figure 2.

The tests included also numerous checks of protection reliability and effectiveness involving 2, 4, 6, 8, and 10 operating anodes. In all tests, both at anchor and underway, the potential was maintained at the protective level and was uniform all over the hull. However, with the current intensity remaining constant the supply voltage (of the automatic static converter [ASC]) increases from 4v for 12 operating anodes to 8v for 2 operating anodes.

To obtain certain current densities for various given potentials, several measurements were made of current densities measured to maintain potentials at 850, 800, and 750mv both at anchor and underway.

The data given in Table 1 show an increase of 50% in the required protective current density with a potential displacement from 750 to 850mv during sailing and a 100% increase when measured at anchor. The voltage increases by 20 and 40% respectively.

Figure 3 reflects the data on the effect of sea water temperatures on the required protective current density level. The tests were run during the Atlantic cruise from the Canary Islands to Cape Town.

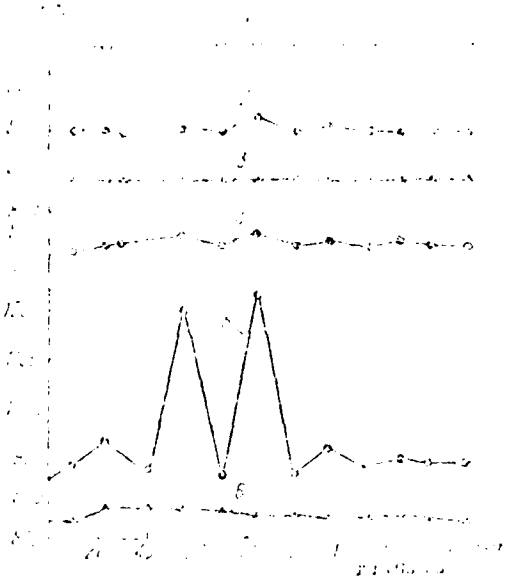

Figure 1. Potential distribution on the underwater hull area over the portable reference electrode prior to the ship going into fresh water (1, 2, 3) and after the ship had been in fresh water (4, 5, 6): 1, 4 -- over the side plating from the waterline to the bilge; 2, 5 -- over the bilge in the anode area; 3, 6 -- over the bottom in the keel area.

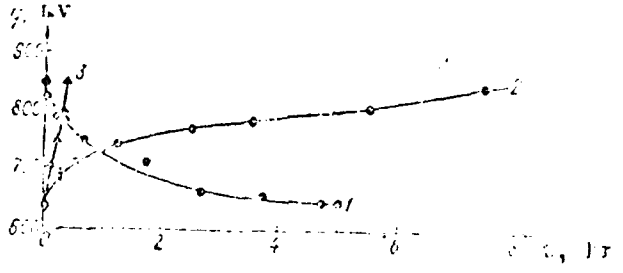

Figure 2. Curve reflecting the protective potential drop rate (after disconnecting the protection system) and its rise to the required value of 850mv.

TABLE 1

Hull Potential, mv	ASC Output Voltage, v	ASC Output Current, a	Protective Current Density a/m^2	Sea Water Temperature °C	Sea Water Salinity 0/00	Ship Speed knots
850	2.5	22	0.0050	28	35	15.75
800	2.2	18	0.0040	28	35	15.70
750	2.0	15	0.0034	28	35	15.70
850	2.0	20	0.0060	24	31	At anchor
800	1.8	12	0.0035	24	31	At anchor
750	1.2	10	0.0030	24	31	At anchor

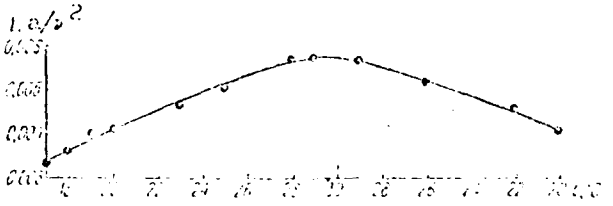

Figure 3. Effect of sea water temperature on the protective current density at 35 0/00 salinity and average speeds of 15 knots.

The data in this figure show that for a constant sea water salinity there is a nearly linear relationship between the temperature on the one hand and the protective current density on the other, at least within 17 to 30 °C.

The effect of sea water salinity on electrochemical protection parameters was studied during the cruise from the Bengal Bay to Calcutta over Hooghley River and to the port Chalna over Pusur River. Because of the tidal flow, the salinity of the river water increased from 3 to 33 0/00 with approaching the bay.

The findings of these studies given in Figure 4 show an abrupt drop of supply voltage when going from fresh water to salt water (Curve 1) and a much slower rise when going from salt water to fresh water (Curve 2), most likely due to films of cathodic deposits formed on the underwater hull area. The protective current density is almost doubled when going from fresh water to salt water and decreases by about the same factor when going from salt water to fresh water.

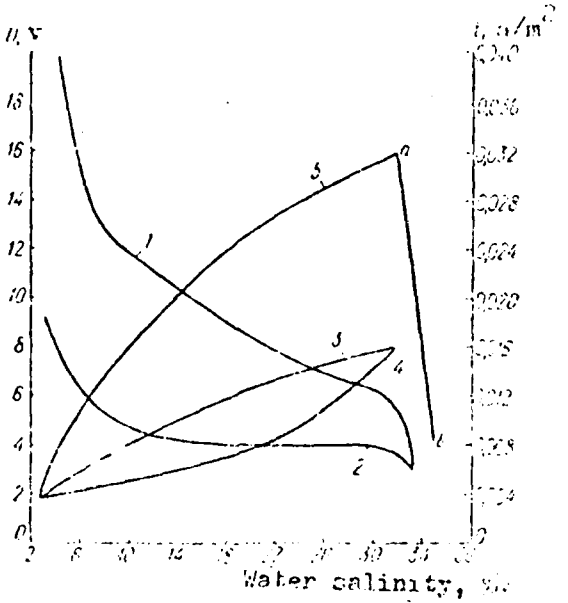

Figure 4. Effect of sea water salinity on the parameters of electrochemical protection with the ship going from fresh water into salt water and conversely.

Curve 5 shows the effect of sea water salinity on protective current density after the ship has been in fresh water for a long time and the subsequent formation of a cathodic film (segment ab, Curve 5) with the ship sailing in sea water at all times.

When the ship stays in fresh water, the cathodic deposits in the paint pores are washed out, the metal is revealed, and the corrosion process becomes activated. The current densities required to suppress these processes with the ship going into a more aggressive environment are many times greater than those required by the ship before going into fresh water. The subsequent decrease of protective density for sailing in sea water (segment ab, Curve 5) indicates restoration of the cathodic film.

The tests included current intensity measurements between the propeller and the hull using the zero resistance method which eliminated voltage drops due to resistances in moving contacts and in equipment. The measurements included also propeller potentials under various conditions of effective protection at various ship speeds. The current between the propeller and the hull can be measured only during shaft rotation when there is an oil wedge (with some resistance) between the bearing and the shaft.

The data on propeller potentials and current flowing between the propeller and the hull under various conditions of electrochemical protection and ship speeds are cited in Table 2. Analysis of these data that the current recorded between the propeller and the hull is the higher the greater the potential difference between the propeller and the hull. The magnitude of this current fluctuated (during the test period) within 1-2a. The potential difference between the propeller and the hull varied from 50 to 200mv in all these tests.

The operating tests conducted on the motor ship KAPITAN PLAUSHEVSKIY have demonstrated that cathodic protection together with painting provide reliable protection of the underwater hull area against corrosion damage. The protective current density for an 850mv hull potential was 0.004-0.007 a/m^2. In some instances after the ship had been sailing in fresh water, the protective current density increased to 0.02-0.03 a/m^2.

TABLE 2

	1	2	3	4	5	6	7	8	9	10	11
12	[illegible]	[illegible]	19,9	12	15,0	[illegible]	—	850	140	1,2	0,[illegible]
13	7/XII	[illegible]	11,9	12	15,0	[illegible]	0,0030	850	40	1,0	0,0[illegible]
14	7/XII	Мраморное море	11,9	12	25,0	870	0,0025	810	70	1,1	0,087
15	7/XII	Дарданеллы	10,3	11	37,0	840	0,0045	810	60	1,2	0,093
16	8/XII	Эгейское море	11,0	17	39,5	[illegible]	0,0080	730	120	1,6	0,125
17	9/XII	Средиземное море	11,5	20	36,5	850	0,0035	740	120	1,7	0,131
18	13/XII	Атлантический океан (Марокко)	15,0	19	36,5	860	0,0030	750	110	1,5	0,117
19	15/XII	Атлантика (Канарские острова)	15,2	24	36,0	850	0,0036	700	150	1,3	0,102
20	19/XII	Атлантика (район Зеленого Сахара)	15,7	25	35,5	850	0,0050	710	140	1,3	0,102
21	22/XII	Гвинейский залив (экватор)	15,6	29	34,0	830	0,0057	710	140	1,5	0,117
22	23/XII	Гвинейский залив (район Конго)	15,15	26	35,0	850	0,0046	710	140	1,5	0,117
23	25/XII	Атлантика (район Анголы)	11,0	20	36,0	850	0,0041	700	100	1,2	0,093
24	29/XII	Атлантика (район Кейптауна)	15,4	29	35,0	830	0,0041	790	40	0,7	0,055
25	31/XII	Индийский океан	15,7	22	34,0	850	0,0046	770	110	1,5	0,117
26	1971 г. 3/I	Индийский океан (район о. Мадагаскар)	15,1	27	34,0	860	0,0058	840	20	0,5	0,004
27	8,1	Индийский океан (экватор)	15,75	28	35,0	800	0,0050	700	100	2,0	0,160
28	12,1	Аравийское море	Стоянка в п. Бомбей	28	35,6	850	0,0030	850	—	—	—
29	30/I	» »	14,3	26	35,0	850	0,0240	830	20	0,5	0,004
30	31/I	» »	17,35	26	35,0	850	0,0170	700	190	2,2	0,172
31	1/II	Индийский океан (район Цейлона)	15,85	27	35,0	850	0,0130	650	200	2,7	0,210
32	3/II	Бенгальский залив	16,5	27	30,5	850	0,0092	650	200	2,5	0,195
33	5/II	» »	Стоянка	23	31.0	850	0,0060	850	—	—	—
34	13/II	» »	14,55	24,5	32,0	850	0,0100	670	110	0,9	0,070
35	14/II	Р. Нусур *	11,7	23	20,0	850	0,0089	800	—	—	—
36	16/II	Р. Нусур	13,7	23	7,0	850	0,0050	720	130	0,6	0,050
37	26/II	Бенгальский залив	14,45	26	30,5	850	0,0320	630	220	1,8	0,140
38	3/III	» »	15,0	28	34,5	850	0,0180	680	170	1,5	0,117

TABLE 2

39	15/III	Индийский океан (в районе Цейлона)	14,0	29	35,0	860	0,0083	660	200	0,8	0,091
40	23/III	Мозамбикский пролив	13,6	29	34,5	860	0,0073	—	—	—	—
41	27/III	Индийский океан (район ЮАР)	14,8	20	34,0	860	0,0065	730	130	1,5	0,117
42	29/III	Атлантический океан (район ЮАР)	15,1	20	35,0	850	0,0073	700	120	1,0	0,080
43	5/IV	Гвинейский залив (район Конго)	15,8	28	35,0	850	0,0083	660	200	2,3	0,180
44	9/IV	Атлантика (район Марокко)	15,4	17	37,0	850	0,0055	660	200	—	—
45	10/IV	Гибралтар	15,5	16	36,5	850	0,0052	—	—	—	—
46	11/IV	Средиземное море (район Алжира)	17,2	15	37,5	870	0,0017	670	200	—	—
47	12/IV	Тунисский пролив	17,4	15	39,0	850	0,0017	650	180	—	—
48	16/IV	Черное море	15,0	10	18,0	850	0,0034	—	—	—	—
49											

* С 6 по 13 февраля 1971 г. защита выключена. Стоянка в Калькутте, пресная вода. С 16 по 27 февраля стоянка в Чалне, пресная вода.

Legend for Table 2:

1) Date
2) Navigational region;
3) Ship speed, knots;
4) Sea water temperature, °C;
5) Sea water salinity, 0/00;
6) Hull potential, mv;
7) Protective current density, a/m^2;
8) Propeller potential, mv;
9) Propeller-hull potential difference, mv;
10) Current between propeller and hull, a;
11) Arbitrary density of protective current on propeller, a/m^2;
12) Black Sea
13) Bosporus
14) Marmara Sea
15) Dardanelles
16) Aegean Sea
17) Mediterranean Sea

Legend for Table 2:

18) Atlantic Ocean (Morocco)
19) Atlantic (Canary Islands)
20) Atlantic (West Sahara region)
21) Guinea Bay (Equator)
22) Guinea Bay (Congo region)
23) Atlantic (Angola region)
24) Atlantic (Cape Town region)
25) Indian Ocean
26) Indian Ocean (Madagascar region)
27) Indian Ocean (Equator)
28) Arabian Sea
28a) Bombay anchorage
29) Arabian Sea
30) Arabian Sea
31) Indian Ocean (Ceylon region)
32) Bengal Bay
33) Bengal Bay
33a) Bengal Bay anchorage
34) Bengal Bay
35) Pusur River
36) Pusur River
37) Bengal Bay
38) Bengal Bay
39) Indian Ocean (Ceylon region)
40) Mozambique Strait
41) Indian Ocean (R.S.A. region)
42) Atlantic Ocean (R.S.A. region)
43) Guinea Bay (Congo region)
44) Atlantic (Morocco region)
45) Gibraltar
46) Mediterranean Sea (Algiers region)
47) Tunisian Strait
48) Black Sea
49) From 6 to 13 February 1971 -- protection disconnected.
Calcutta anchorage -- fresh water.
From 16 to 27 February 1971, Chalna anchorage, fresh water.

EFFECTIVENESS OF ELECTROCHEMICAL PROTECTION OF 25L STEEL AGAINST CORROSION CAVITATION IN FLOWING SEA WATER

[By G. K. Gavrskiy, N. I. Yermolenko, Yu. Ye. Zobachev (Candidate of Technical Science), A. V. Kurdin (Candidate of Technical Science), Yu. V. Luk'yanova, and R. N. Metel'skaya. TRANSACTIONS of the Central Scientific Research Institute of the Maritime Fleet. Technical Operations of the Maritime Fleet. Thermochemical Studies. Corrosion and Fouling Control. Transport Publishing House, Leningrad, 1972, No. 160, pp. 38-46; Russian]

Earlier works [1-4] dealt with the feasibility of using electric current applications for protecting metal structures against the effects of corrosion cavitation both in river and sea waters. These studies concerned the effectiveness of electrochemical protection of metals in the case of highly developed cavitation, i.e. when the mechanical effects predominate over the chemical effects (corrosion).

For practical purposes and the solution of relevant problems, it is of interest to determine the feasibility of applied current protection against moderate cavitation, i.e. when the mechanical effects and the chemical effects are commensurate.

Within the last three years the Far Eastern Branch of the Central Scientific Research Institute of the Maritime Fleet has been conducting investigations on the effectiveness of electrochemical protection of 25L carbon steel against corrosion cavitation damage in sea water at flow velocities of 24 to 32 m/sec corresponding to the linear velocity of a propeller blade edge in modern vessels.

The tests have been conducted with the aid of specially designed units: a diffuser and a jet blower. Both units were used for testing the specimens in sea water at flow velocities of 24 to 32 m/sec. The flow of water in the diffuser was produced by an ordinary pump, while that in the jet blower -- by a centrifugal force produced by rotating a spindle with the test specimens on it. The cavitation effect in the diffuser was produced by special barriers in the flow channel; in the jet blower, cavitation bubbles were produced by placing the specimens at a specific angle to the water current. Both these units described in [4] were supplemented in this experiment with an electrochemical measuring device (figure 1). The specimens were polarized by a steel electrode. A P-307 potentiometer was used for voltage measurements. A

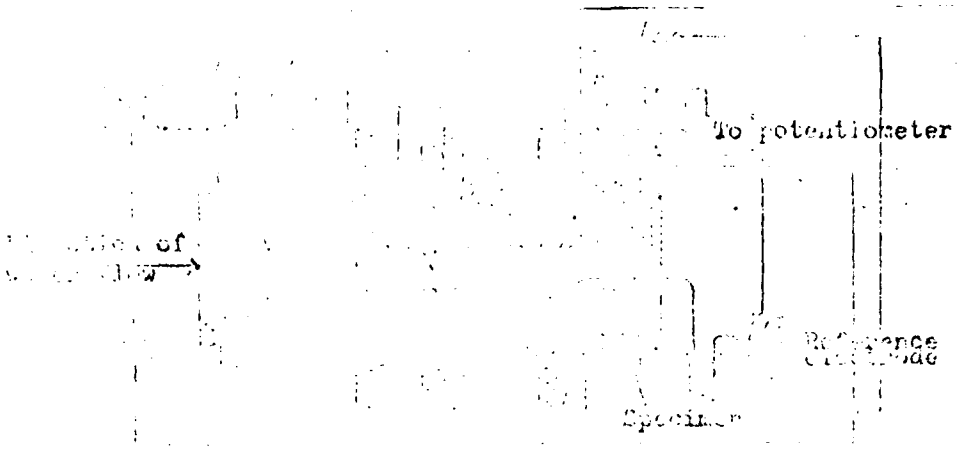

Figure 1. Diffuser-type testing unit with an electrochemical measuring circuit.

calomel-loaded reference electrode was used in all cases. The testing lasted 100 hours.

Table 1 shows the test results.

It was demonstrated within these 100 hrs of testing of 2.5L steel at flow velocities of 32 m/sec that protective current decreases with time.

The protective current produced by 10-a/m^2 polarization for Curve 1 is 2540 μa (curve intersection point with straight line A - A corresponding to a 0.660-v potential); after 30 hours of polarization, the protective current decreases to 582 μa. Subsequently, the protective current decreases at a slower rate. Thus, after 50 hours of polarization, the protective current is 550 μa, after 75 hours -- 496 μa, and after 100 hours, the protective current is 441 μa.

Polarization with current of 2.5 a/m^2 (Figure 2,b) at flow velocities of 32 m/sec causes a slightly lesser change in protective current with time. Thus, 30 hours of polarization with 10-a/m^2 current decreases the protective current by a factor of 4.36, while polarization with 2.5-a/m^2 current within the same number of hours decreases the protective current by a factor of 4.3 (from 2540 to 590 μa.)

TABLE 1

1	2	3	4	5	6
0	[illegible]	2,61	[illegible]	0	0
	[illegible]	1,30	[illegible]	0	0
	21	1,10	3,21	0	0
	16	[illegible]	1,57	0	0
0,5	[illegible]	[illegible]	[illegible]	42,1	40,2
	[illegible]	[illegible]	2,71	45,2	43,1
	[illegible]	[illegible]	1,77	46,8	[illegible]
	16	[illegible]	1,62	[illegible]	35,0
0,7	[illegible]	1,28	[illegible]	[illegible]	[illegible]
	[illegible]	0,78	[illegible]	[illegible]	15,9
	[illegible]	[illegible]	[illegible]	[illegible]	[illegible]
	[illegible]	[illegible]	[illegible]	[illegible]	[illegible]
[illegible]	[illegible]	[illegible]	[illegible]	[illegible]	[illegible]
	[illegible]	0,71	[illegible]	[illegible]	[illegible]
	[illegible]	[illegible]	[illegible]	34,1	[illegible]
	[illegible]	[illegible]	0,97	[illegible]	[illegible]
[illegible]	[illegible]	[illegible]	[illegible]	[illegible]	[illegible]
	[illegible]	[illegible]	[illegible]	[illegible]	[illegible]
	21	[illegible]	[illegible]	[illegible]	[illegible]
	[illegible]	[illegible]	[illegible]	[illegible]	[illegible]
[illegible]	[illegible]	[illegible]	[illegible]	[illegible]	[illegible]
	[illegible]	[illegible]	[illegible]	[illegible]	[illegible]
	[illegible]	[illegible]	[illegible]	[illegible]	[illegible]
	16	[illegible]	[illegible]	[illegible]	[illegible]
10,0	[illegible]	0,57	[illegible]	[illegible]	[illegible]
	[illegible]	0,28	[illegible]	[illegible]	[illegible]
	21	[illegible]	[illegible]	[illegible]	[illegible]
	16	[illegible]	[illegible]	15,6	[illegible]

[illegible]	[illegible]	[illegible]	[illegible]	[illegible]	[illegible]
	[illegible]	0,1	1,[illegible]	[illegible],0	[illegible],0
	[illegible]	0,[illegible]	[illegible],[illegible]	[illegible],[illegible]	81,0
	[illegible]	0,17	[illegible],[illegible]	81,5	84,0
	16	0,21	[illegible],[illegible]	87,4	90,0
[illegible]	[illegible]	0,24	0,[illegible]	91,2	93,2
	[illegible]	0,12	[illegible],[illegible]	91,[illegible]	95,1
	[illegible]	0,08	[illegible],[illegible]	92,8	91,7
	[illegible]	[illegible],[illegible]	[illegible],[illegible]	[illegible],1	[illegible],[illegible]

Legend for Table 1:

1) current density, a/m^2;
2) flow velocity, m/sec;
3) weight loss, $g/m^2 \cdot hr$;
4) degree of protection, %;
5) diffuser;
6) jet blower.

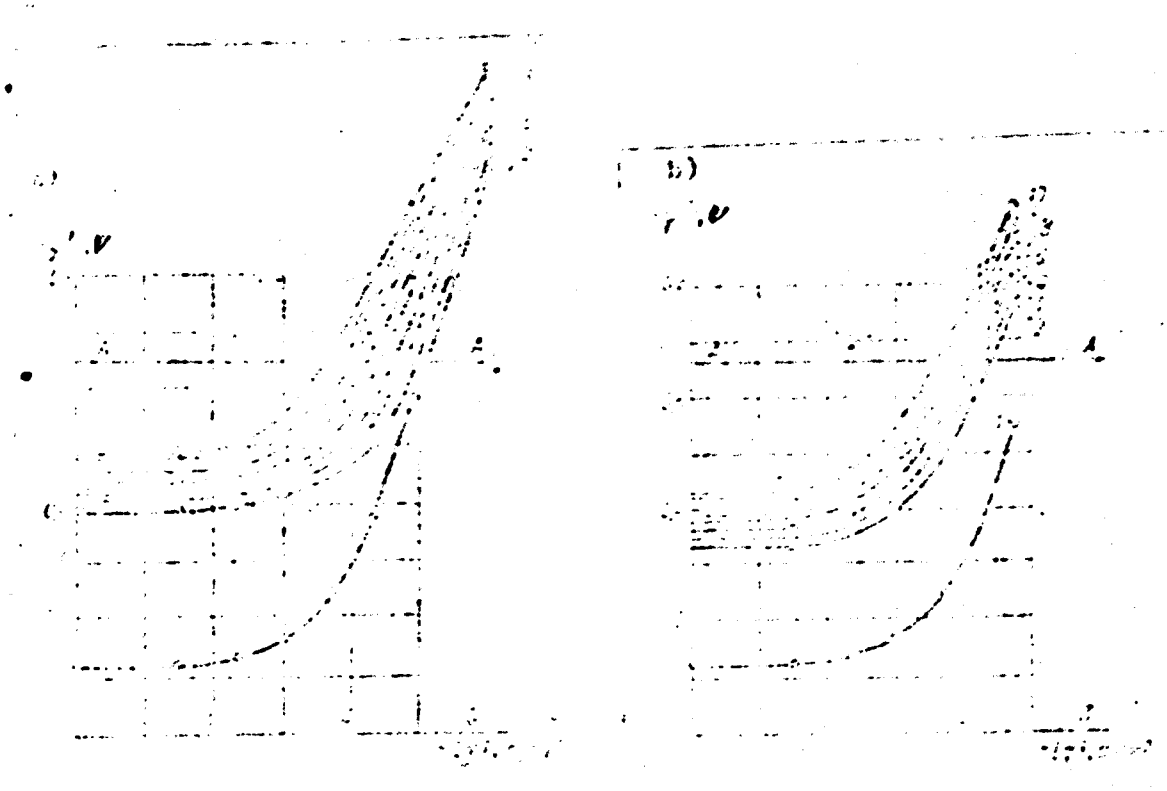

Figure 2. Cathodic polarization curves of 25L steel plotted during polarization: a) 10-a/m^2 current; b) 2.5-a/m^2 current.

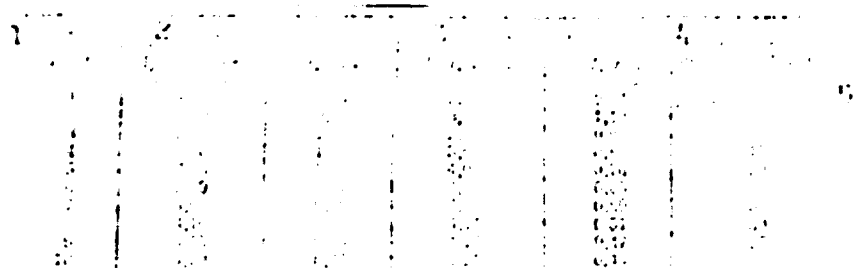

Legend for Table:

1) No. of curve;
2) Figure 2,a;
3) Figure 2,b;
4) polarization time, hrs;
5) without polarization.

About the same relationships were obtained in tests on specimens at other flow velocities. At 28 m/sec and a 10-a/m^2 current there is a decrease in protective current as a function of specimen polarization time. Thus, if the protective current was 1750 μa (at the beginning of the experiment), it decreased after 5 hrs of polarization to 1270 μa. After 30 hrs, the protective current was as low as 353 μa which is one fifth of its initial value. For the same flow velocity and a polarization current of 2.5 a/m^2, however, the protective current decreases at a slightly lower rate: at the beginning of the experiment it was 1780 μa, after 5 hrs -- 840 μa, and after 30 hrs it was 420 μa, i.e., 4.4 times less than its initial value. The results of these tests are given in Table 2.

The table shows that the protective current reduction factor for polarization with 10-a/m^2 current, with a decrease in flow velocity, increases from 4.36 for 32 m/sec to 6.15 for 24 m/sec. This may be attributed to the fact that a stronger cavitation decreases the effectiveness of the hydrogen cushion whose damping properties (for this current density) are those that produce the protective effect. When polarization is effected with a 2.5-a/m^2 current, hydrogen is liberated to a lesser degree; the film which is formed during polarization removes itself

TABLE 2

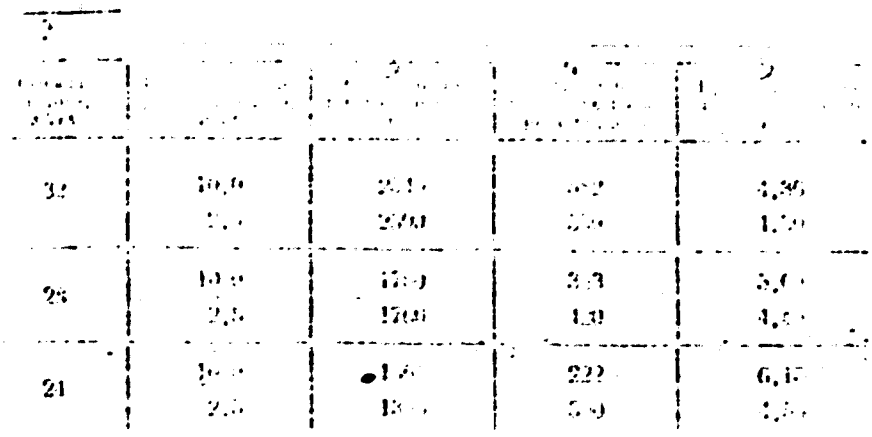

Legend for Table 2:

1) flow velocity, m/sec;
2) polarization current density, a/m^2;
3) protective current at the beginning of the test, μa;
4) protective current after 30 hrs of polarization, μa;
5) reduction factor of protective current.

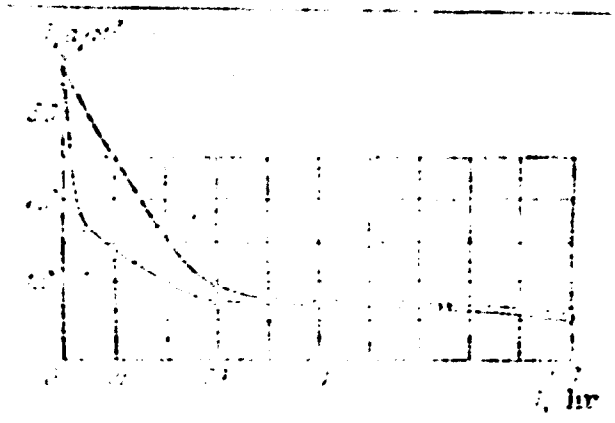

Figure 3. Protective current densities as a function of polarization time with 10 a/m^2 (1) and 2.5 a/m^2 at a flow velocity of 32 m/sec.

at flow velocities of 28 and 32 m/sec; the protective current build-up factor, therefore, changes only slightly for all flow velocities (from 4.30 for 32 m/sec to 4.55 for 24 m/sec.

The protective currents as a function of polarization time were calculated from the curves plotted during specimen polarization with 10- and 2.5-a/m^2 currents. The results are given in Figure 3.

It was observed (at all experimental flow velocities) that polarization with 2.5-a/m^2 current produced a hydroxide film on the specimens' surface (except for cavitation-affected areas) while there were no films on specimens polarized with 10-a/m^2 current. This suggests that protection is governed by various mechanisms of current effects: for a 10-a/m^2 current density, the potential is 1 v at which point there begins abundant liberation of hydrogen on the specimen's surface hindering film formation. The fairly high degree of protection is attributed to the beneficial effect of the hydrogen cushion on the specimen's surface.

For 2.5-a/m^2 current densities the potential is 0.660 v. It was observed that the films that were formed in flowing water were much weaker than those produced in calm water (even with polarization currents being many times lower than those for specimens in flowing water). Polarization of specimens with 10-a/m^2 current for 25 hrs in calm water and then 75 hrs in flow has shown that the cathodic films (though very weak) that have been formed during polarization in calm water are readily destroyed in flowing water regardless of its velocity. In a similar experiment involving 2.5-a/m^2 current the percentage of film preservation after 25 hrs of testing in flow was much higher, it was also shown that polarization in calm water with 0.4-a/m^2 current yields an equally strong film (Figure 4). The film forming time in the latter case was 25 hrs. Figure 4 shows that film formation is at its minimum when produced under 0.4-a/m^2 current. This observation seems

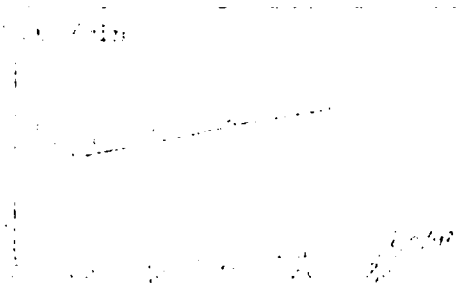

Figure 4. Potential variation rate of the steel specimen after disconnecting the polarization current (flow velocity, 32 m/sec). Polarization done in calm water.

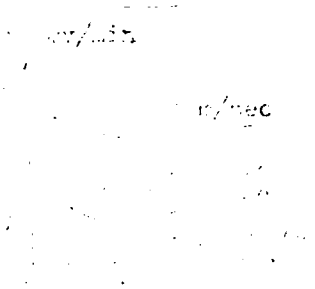

Figure 5. Potential variation rate of the steel specimen as a function of polarization current density.

to be of prime importance since it permits a more economical rating of power in designing electrochemical protection systems.

For specimens that have not been treated for pre-polarization, the optimum conditions for film forming were produced with current densities of 1.5-2.5 a/m^2. This conclusion has been corroborated by studies on changes in stationary potentials as a function of time after disconnecting the polarizing current (Figure 5). The film forming time was 100 hrs. Figure 5 shows that the minimum of $\Delta\varphi$ falls on deposits formed at current densities of 1.5-2.5 a/m^2. The comparison of curves in Figure 4 and Figure 5 shows that variations of flow velocities produce considerable changes in film forming. Thus, if the optimum current density for calm water is 0.4 a/m^2, a flow velocity

of 32 m/sec would require 1.5 a/m^2. The potential increment (for a flowing electrolyte) is attributed basically to the mechanical effect of sea water flow hindering the formation of protective films. The marked reduction in the protective current is attributed to the growth of the cathodic film which leads to screening the specimen's surface. This increases the true current while decreasing the total protective current. Termination of film growth (after 25-30 hrs of polarization) suspends the drop of protective current.

Conclusions

1. Electrochemical protection is an effective means of increasing the resistance of carbon steel to corrosion cavitation in sea water.

2. For sea water flow velocities ranging from 24 to 32 m/sec and corresponding to the linear velocities of propeller blade edges in modern ships, considerable changes in the degree of protection occur only for polarization current densities ranging from 0.5 a/m^2 to 10 a/m^2 (42 and 77%, respectively).

3. The protective current markedly decreases as a function of time at all flow velocities.

4. Prepolarization of specimens in calm water reduces considerably the protective current during subsequent testing in flowing water.

REFERENCES

1. Glikman, L.A. and Zobachev, Yv. Ye. Vliyaniye katodnoy polyarizatsii na kavitatsionnuyu stoykost' uglerodistoy stali (Effect of Cathodic Polarization on the Resistance of Carbon Steel to Cavitation). "Metallovedeniye i termicheskaya obrabotka metallov", No. 4, 1956.

2. Len'kova, L.N., Vysotskiy, A.A. and Zobachev, Yv. Ye. Elektrokhimicheskaya zashchita metallov ot kavitatsionnogo vozdeystviya vysokoy intensivnosti (Electrochemical Protection of Metals Against Highly Intensive Cavitation). Inf. sb. TsNIIMFa, No. 49 (149). Moscow. Central Office of Scientific and Technical Information of the USSR Ministry of the Maritime Fleet, 1967.

3. Kurdin, A.V., Luk'yanova, Yv. V., Vysotskiy, A.A. and Zobachev, Yv. Ye. Elektrokhimicheskaya zashchita ot kavitatsionnogo razrusheniya razlichnoy intensivnosti (Electrochemical Protection Against Cavitation Damage of Varying Intensity). TR. TsNIIMFa, No. 116, Leningrad, "Transport" Publishing House, 1969.

4. Kurdin, A.V. Issledovaniye povedeniya materialov grebnykh vintov i nekotorykh sposobov zashchity ikh v usloviyakh korrozionno-mekhanicheskogo vozdeystviya morskoy vody (Behavior of Propeller Materials and Certain Methods of Protection on Exposure to Corrosive and Mechanical Effects of Sea Water). Author's Abstract of Dissertation for the Candidate degree of Technical Sciences, Vladivostok, 1970.

3. Kurdin, A.V., Luk'yanova, Yv. V., Vysotskiy, A.A. and Zobachev, Yv. Ye. Elektrokhimicheskaya zashchita ot kavitatsionnogo razrusheniya razlichnoy intensivnosti (Electrochemical Protection Against Cavitation Damage of Varying Intensity). TR. TsNIIMFa, No. 116, Leningrad, "Transport" Publishing House, 1969.

4. Kurdin, A.V. Issledovaniye povedeniya materialov grebnykh vintov i nekotorykh sposobov zashchity ikh v usloviyakh korrozionno-mekhanicheskogo vozdeystviya morskoy vody (Behavior of Propeller Materials and Certain Methods of Protection on Exposure to Corrosive and Mechanical Effects of Sea Water). Author's Abstract of Dissertation for the Candidate degree of Technical Sciences, Vladivostok, 1970.

DISTRIBUTION OF HIGH-FREQUENCY VIBRATION IN HULLS OF KRASNOGRAD-CLASS SHIPS EQUIPPED WITH ULTRASONIC ANTIFOULING PROTECTION SYSTEMS

[By P.S. Sheherbakov, F. Ye. Grigor'yan, and N.V. Pogrebnyak. TRANSACTIONS of the Central Scientific Research Institute of the Maritime Fleet, TECHNICAL OPERATION OF THE MARITIME FLEET. THERMOCHEMICAL STUDIES. CONTROL OF CORROSION AND FOULING. Transport Publishing House, Leningrad, 1972, No. 160, pp. 68-72; Russian]

Ultrasonic protection has been used in the last few years to reduce fouling of underwater hull parts. The maritime fleet has now about 20 vessels equipped with ultrasonic antifouling protection systems. Despite the fact that the latter have been in use for over 10 years, there are still no data on the distribution of high-frequency vibrations over hull structures.

The objective of this study was to check the efficiency of ultrasonic antifouling protection and study of vibration damping in the hull by measuring high-frequency vibrations on a KRASNOGRAD-CLASS ship.

The ultrasonic system on these ships incorporates a vacuum tube ultrasonic oscillator with a 200-w power output and four more oscillators. The oscillator's output voltage frequency varies within 17-30 KHZ. The oscillator uses a self-excitation, and frequency-modulation circuit.

The magnetostriction oscillator consists of four nickel plates assembled in a package and soldered to a steel prism which is welded to the inner side of the hull plating. The plates carry a winding in which a variable magnetic field is produced. Under the effect of the magnetic field, the plate package, possessing a magnetostriction property, undergoes periodic changes in size. The vibrations of the package are transmitted through the prism (waveguide) to the outer hull plating.

Measurements of the oscillation acceleration amplitude levels were conducted on KRASNOGRAD-CLASS motor ships using Danish measuring equipment of the firm Bnuel and Kjaerw. The 4331-model Danish pickup with a linear acceleration frequency characteristic up to 60 KHZ was used as the ultrasonic vibration detector. A microphonic amplifier with an octave filter and a linear frequency characteristic up to 40 KHZ was used as the measuring device.

The figure below shows measurements of vibrations produced by an ultrasonic protection exciter in the second bottom area on KRASNOGRAD motor ships both during dockup and while afloat. It is shown that the vibration level along the ship hull decreases with an increase in distance from the vibration source (exciter). In the immediate vicinity of the radiator installation site (3-5m from the source) the damping decreases by 20% due to energy losses in hull structures and sound radiation to the water. When waves propagate through bulkheads, abrupt damping is observed.

The data obtained are in some variance with those in study [1].

A dock inspection of KRASNOVRAL'SK and KLIN motor ships in June 1970 corroborated the authors' assumption on vibration insulation in the bulkheads. Along the hull sides there were fine balanus strips at the weld areas of the bulkheads and framing to the hull (at minimum vibration areas) forming a typical "zebra pattern".

At a considerable distance from the exciters -- an area where the oscillation acceleration level was below 70 db -- there was a dense balanus population. This shows that it would be impossible to ensure a fairly uniform vibration level along the entire hull and a good protection against fouling even if this method has its advocates [2, 3].

A comparative analysis of the operation of ultrasonic protection on KRASNOGRAD-CLASS ships and those on project 394 (under the Central Scientific Research Institute of Transportation Construction) has shown the same pattern of ultrasonic vibrations to be true for ships of different displacements.

In order to determine the operating effectiveness of ultrasonic systems, the Central Scientific Research Institute of the Maritime Fleet conducted vibration studies in the oscillator areas on all ships equipped with such systems.

The findings are presented in Tables 1 and 2.

As shown by the measurements the difference in the numerical values of vibration ranges within 25 decibels; all ships used the same type of equipment. The difference is attributed to misalignment of the TTAGD oscillator tube systems of the power amplifier during operation.

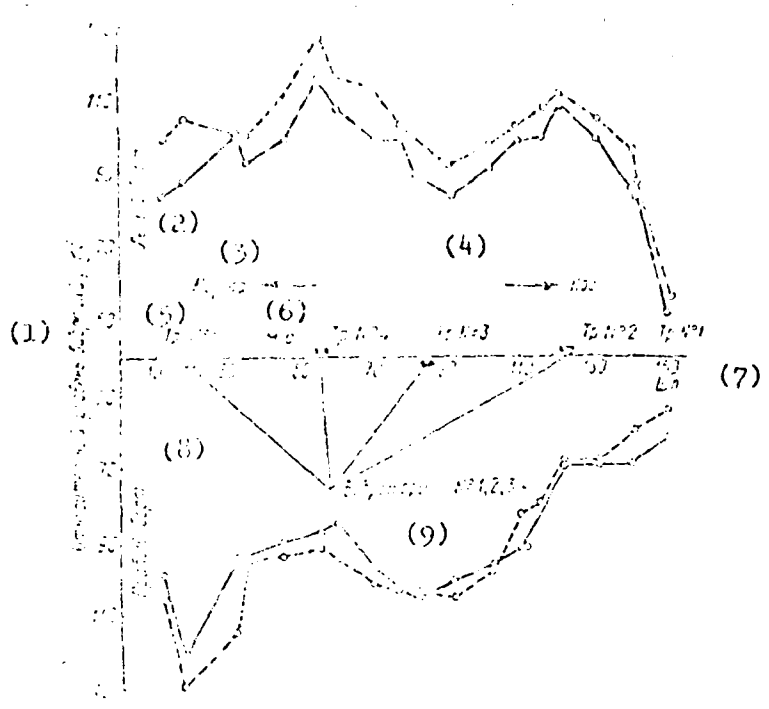

Distribution of ultrasonic vibrations along the length of the KRASNOGRAD motor ship measured in the second bottom area:

----- during docking; ——— while afloat

Legend:
(1) relative vibration level, db;
(2) larboard side;
(3) stern;
(4) bow;
(5) Transom No. 5;
(6) observation site;
(7) Framing;
(8) starboard side;
(9) Oscillators

The results obtained here show that the hull vibration level of ships having ultrasonic protection in the acceleration frequency band of 16 KHZ remains within the 100-120 db range.

TABLE 1

Name of Ship	Vibration level on KRASNOGRAD-class ships in the oscillator area, 16 KHZ octave band, db					
	(larboard side)			(starboard side)		
	200 mm above the oscillator	1 m toward the stern	2 m toward the stern	200 m above the oscillator	1 m toward the stern	2 m toward the stern
KRASNOYE SECO	124.0	119.0	101.5	113	100.5	108.0
KALININABAD	119.0	110.0	105.0	115	105.0	102.0
KRASNOKAMSK	120.0	110.0	105.0	113	106.0	103.0
KANEV	113.0	100.0	100.0	105	95.5	90.0
KIMOVSK	122.0	113.5	116.0	117	106.0	103.5
KLIN	128.5	112.5	-	-	94.5	-
KRASNOORAL'SK	115.0	107.5	-	110	102.0	-

TABLE 2

Name of Ship	Vibration level on MICHVRINSK-CLASS SHIPS in the oscillator area 16-KHZ octave band, db			
	larboard side (bow)	larboard side (stern)	starboard side (bow)	starboard side (stern)
CHERNYAKHOVSK	107	113.5	123	91.5
L'GOV	94.5	85.5	104.5	112
IZHEVSK	NONE	85.5	NONE	83

Conclusions

1. The structural rigidity of the hull affects vibration distribution along the hull. In placing the oscillators, one must take into consideration the vibration insulation and damping properties of the various hull areas.

2. Ultrasonic vibrations within 115-125 db reduce considerably the fouling of the underwater parts of the hull.

REFERENCES

1. Kornev, V.V. Fizicheskiye zadachi ul'trazvukovoy zashchity sudov ot obrastaniya (Physical Problems of Ultrasonic Antifouling Protection of Ships). Author's Abstract of Dissertation for the Degree of Candidate of Technical Sciences. LKI (Leningrad Shipbuilding Institute) 1965.

2. Aksel'band, A.M. Vliyaniye ul'trazvukovykh kolebaniy na processy obrastaniya korpusov sudov i na morskiye obrastaniya (Effect of Ultrasonic Vibration on Fouling of Ship Hulls). Tekhnologiya sudostroyeniya, No. 5, 1964.

3. Subkbew, H.J., Schultz, S. Schiffbantechnik, V.3, No. 7, 1963.

STUDY OF THE VOLTAIC COUPLE HULL-PROPELLER

[Yevdokimov, O.V. and Shcherbakov, P.S.; Central Scientific Research Institute of the Maritime Fleet, Transactions, Technical Operations of the Maritime Fleet. Thermochemical Studies. Corrosion and Fouling Control, No. 160, p. 72-78; "Transport" Publishing House, Leningrad, 1972; Russian]

The most intensive source of current on the underwater hull portion is the voltaic couple hull-propeller.

Quantitatively, the galvanic current of this couple may be determined by the formula

$$I_{h.pr} = \frac{U_h - U_{pr}}{R_{le} + R_{in} + R_h + R_{pr} + R_{pa}}, \qquad (1)$$

where R_{le} is the propeller leakage resistance; R_{in} is the internal resistance of the bearings; R_{pa} is the paint resistance; R_h and R_{pr} are hull and propeller polarization resistances, respectively; $U_h - U_{pr}$ is the potential difference between the hull and the propeller.

The values of the terms in Formula (1) are determined from the following expressions:

The propeller leakage resistance

$$R_{le} = \frac{1}{\gamma r_o} \cdot \frac{K(k)}{K(k')}, \qquad (2)$$

where γ is the electroconductivity of water, 1/ohm·m;

r_o is the propeller radius, m;

$K(k)$; $K(k')$ are the complete elliptic integrals of the first kind with moduli $K = h_o - r_o/h_o + r_o$ and $k' = \sqrt{1 - K^2}$, respectively;

h_o is the distance from the center of the propeller to the ship hull along the normal to the axis of the shafting, m.

The hull polarization resistance

$$R_h = B_{pr}/S_{pr} \qquad (3)$$

where B_{pr} is the specific polarizability of the propeller (in ohm·m^2) which is 0.3 for a ship in motion and is 7.7 at anchorage; S_{pr} is the propeller surface, m^2.

The internal resistance of the shaft line represents a system of parallel resistances of journal bearings.

The resistance of a single bearing is determined from the following formula

$$\frac{1}{R} = G \cdot \gamma_o \left| \frac{\quad}{\quad} \right. \qquad (4)$$

where γ_o is the electric conductivity of the oil; h is the clearance between the shaft and the bush, m; r_1, r_2 are the radii of the shaft and the bush, m;

$h \geq (3 \text{ to } 8)[H_{sh} + H_{bn}]$;

H_{sh}; H_{bn} are the mean square heights of the shaft surface roughness and that of the bush, respectively.

The total resistance of the internal circuit

$$R_{in} = \sum R_i = \sum \frac{1}{G_i}$$

The effective current values may be determined graphically if we know the so-called internal curve of the voltaic couple hull-propeller representing a slightly modified polarization curve in which the abscissa axis reflects the current and the Y-axis--the potential difference between the hull and the propeller. Then by measuring the effective voltage between the shaft and the hull ΔU_e and using the diagram in Figure 1, we can determine

the current value of the hull-propeller couple. The tangent of the inclination angle of a straight line drawn through both the origin of the coordinates and the operating point determines the resistance of the internal

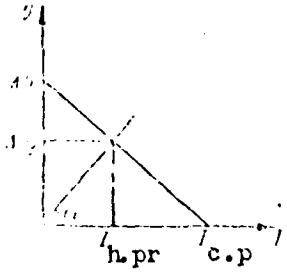

Figure 1. Characteristic of the voltaic couple hull-propeller

section of the circuit (the stern and journal bearings.

The diagram may be plotted according to a method cited in study [1]. The table below gives hull-propeller couple current values for various types of ships measured by an ammeter circuit with zero resistance. The measurements indicate that the current value depends on many factors, such as propeller material, water salinity and temperature, the number of protectors installed on the hull, and the state of paint on the underwater portion of the hull.

If we recalculate the obtained data to current density on the propeller after connecting it electrically with the hull, then the current density values will be 0.1-0.12 a/m^2 for carbon steel propellers; 0.2-0.25 a/m^2 for stainless steel propellers; and, 0.5-1.5 a/m^2 for propellers of LMHzZh-55-3 brass.

The above short-circuit current measurements correspond to the maximum corrosion current produced between the hull and the propeller. Hence, in order to eliminate hull corrosion and provide propeller protection, it is necessary to ensure equality between the current of contact corrosion and that of protection.

It should be noted that the basic operating criterion for a voltaic couple are the resistance relationships between the electrodes. Specifically, application of external current results in potential redistribution over the electrode

Ship's Name	Electrode Potential Difference, mv		Current Intensity $I_{c.p}$ a	Propeller Material	Water Salinity 0/00	Sea water Electric Conductivity 1/ohm.m	Propeller diameter, m
	U max (According to manual)	U_e (on ship)					
ALATYR'LES	400	230	14.0	NOVOSTON	37	5	4.6
BOBRUYSKLES	400	300	14.5	NOVOSTON	37	5	4.6
KIROV	400	260	6.8	LMtsZh 55-3-1 (Brass)	18	2	5.8
VLADIMIR	400	190	6.1	Same	18	2	5.8
VINNITSA	100	70	2.6	St. 25L	18	2	5.8
NORDVIK	120	160	3.5	St. 1X14ND	34	5	4.5
DZHORDANO BRONO	400	200	14.8	NIAL'MA	18	2	6.6
OKTABR'SKAYA REVOLYUTS-IYA	400	290	21.0	NOVOSTON	35	5	6.2
KOLKHIDA	380	260	1.3	LMtsZh 55-3-1 Brass	18	2	2.4
TATARIYA	380	250	7.5	Same	34	5	2.4
KIEV	100	70	2	Steel (3% M)	7	0.6	5.8

Ship's Name	Electrode Potential Difference, mv		Current Intensity $I_{c.p}$ a	Propeller Material	Water Salinity 0/00	Sea water Electric Conductivity 1/ohm.m	Propeller diameter, m
	U max (According to manual)	U_e (on ship)					
ALATYR'LES	400	230	14.0	NOVOSTON	37	5	4.6
BOBRUYSKLES	400	300	14.5	NOVOSTON	37	5	4.6
KIROV	400	260	6.8	LMtsZh 55-3-1 (Brass)	18	2	5.8
VLADIMIR	400	190	6.1	Same	18	2	5.8
VINNITSA	100	70	2.6	St. 25L	18	2	5.8
NORDVIK	120	160	3.5	St. 1X14ND	34	5	4.5
DZHORDANO BRONO	400	200	14.8	NIAL'MA	18	2	6.6
OKTABR'SKAYA REVOLYUTS-IYA	400	290	21.0	NOVOSTON	35	5	6.2
KOLKHIDA	380	260	1.3	LMtsZh 55-3-1 Brass	18	2	2.4
TATARIYA	380	250	7.5	Same	34	5	2.4
KIEV	100	70	2	Steel (3% M)	7	0.6	5.8

surfaces, addition of corrosion current and protection current vectors, and a voltage drop on the internal resistance.

During the cathodic polarization of the hull, a portion of the current is short-circuited to the propeller which leads to a reduction of the electrode potential difference between the propeller and the hull (an increase in polarization resistance R_{p2}) and, consequently, a decrease in the galvanic current of the hull-propeller couple. The amount of current flowing to the propeller is basically determined by the internal resistance of the bearings R_{in} as well as by the location of the cathodic protection anodes. Such a system represents a three-electrode voltaic system whose equivalent circuit is shown in Figure 2.

In this system

1) the journal and stern bearing resistances are replaced by a single equivalent resistance R_{in} connected in series with the source emf;

2) the leakage resistance $R_{a.h}$ (anode-hull) participates fully in the cathodic polarization of the hull. The amount of current flowing to the propeller $I_{a.pr}$ can be ignored.

Figure 2 may be used as a basis for determining currents in various systems using the following formula

$$\begin{cases} (R_{h.pr} + R_{in})\, i_1 - R_{h.pr} i_2 = E_{so}; \\ -R_{h.pr} + (R_{h.pr} + R_{a.pr} + R_{a.h})\, i_2 - R_{a.h} i_3 = 0. \\ -R_{a.h} i_2 + (R_{a.h} + R_{c.p})\, i_3 = E_{c.p} \end{cases}$$

By solving this equation, one may determine the following:

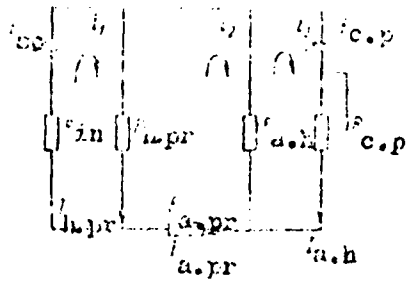

Figure 2. Equivalent circuitry of the hull-propeller system of a ship with cathodic protection

E_{so} -- source emf, i.e. the potential difference of the voltaic couple hull-propeller (U_h-U_{pr}); $E_{c.p}$ -- cathodic protection source emf, i.e. the potential difference between the emf of the cathodic protection source and the effective emf of the couple ΔU produced by the voltaic interaction of the anode with the hull; $E_{c.p} = 0.95\ U_v - \Delta U$ (5% voltage drop in the network; R_{in} -- internal circuitry resistance (for the hull-propeller couple), resistance of journal and stern bearings - the electron conductivity section; $R_{h.pr}$ -- the leakage resistance between the propeller and the hull; $R_{a.h}$ -- the leakage resistance between the anode and the hull; $R_{a.pr}$ -- the leakage resistance between the anode and the propeller; $R_{c.p}$ -- the control resistance in the cathodic protection plate circuit; i_1, i_2, i_3 -- are currents in the various systems.

The current between the hull and the propeller

$$I_{h.pr}=i_1-i_2=\frac{E_{so}[R_{a.pr}R_{a.h}+R_{c.p}(R_{a.h}+R_{a.pr})]-E_{c.p}R_{a.h}R_1}{\Sigma R}; \quad (5)$$

The current between the anode and the hull

$$I_{a.h}=i_3-i_2=\frac{E_{o.p}[R_{a.pr}R_{h.pr}+R_{in}(R_{a.pr}+R_{h.pr})]-E_{so}R_{h.pr}R_{c.p}}{\Sigma R}; \quad (6)$$

The current between the anode and the propeller

$$I_{a.pr}=i_2=\frac{R_{h.pr}(E_{c.p}+E_{so})+R_{a.h}R_{in}E_{c.p}+R_{h.pr}R_{c.p}E_{so}}{\Sigma R}, \quad (7)$$

where $\Sigma R = R_{a.pr}R_{a.h}R_{h.pr} + (R_{h.pr} + R_{a.h} + R_{a.pr})R_{c.p}R_{in} + (R_{a.h} + R_{a.pr})R_{h.pr}R_{c.p} + (R_{h.pr} + R_{a.pr})R_{a.h}R_{in}$.

Analysis of these formulas indicates that when the internal circuit resistance increases and becomes much greater than the resistance of the electrolytic (outboard) section of the circuit $(R_{pr} \gg R_{a.h})_1$ then the current flowing through it exceeds that flowing through the internal section of the circuit. The total resistance increases and the current value $I_{a.pr}$ can be ignored ($I_{a.pr} = 0$).

This is accompanied by polarization processes leading to changes in the potential difference between the propeller and the hull -- a fact that had been repeatedly checked out under operating conditions. Thus, for example, during the cathodic polarization of the motorboat PULKOVO hull, the interelectrode potential difference between the propeller and the hull was 50-70 mv; without cathodic protection the difference was as high as 200 mv.

In this case $R_{in} \gg 0$; $R_{a.pr} > 0$; $I_{a.pr} = i_2 = 0$; using equations (5) and (6) we will obtain

$$I_{a.h} = I_{h.pr}i_3/i_1. \quad (8)$$

If there is a drop in the internal resistance (due to shaft contact, water getting into the bearings, etc.), then the voltage between the shaft and the hull decreases, the current value will exceed zero ($R_{in} \cong 0$; $R_{a.pr} \cong 0$; $I_{a.pr} \neq 0$), and equations (5) and (6) would assume the following form

$$I_{h.pr}=\frac{E_{so}R_{c.p}R_{a.h}}{\Delta}; \quad I_{a.h}=\frac{-E_{so}R_{c.p}R_{h.pr}}{\Delta}.$$

Then

$$I_{a.h}=I_{h.pr}i_3-i_2/i_1-i_2=I_{h.pr}R_{h.pr}/R_{a.h}. \qquad (9)$$

As seen from Formula (9), in the case of a high internal resistance, the greater the difference between the cathodic protection current $I_{a.h}$ and the initial current of the hull-propeller couple, the higher the current $i_3>i_1$ which, in turn, is determined by the relationship between these circuits. When $i_3=i_1$, the current in Formula (8) will be equal. Otherwise this equality is determined by the condition $R_{h.pr}>R_{a.h}$. When $R_{h.pr}=R_{a.h}$, the currents in Formula (9) will be equal. This may be achieved by increasing the resistance $R_{a.h}$ which, in turn, can be effected by using a larger anodic shield.

The journal bearings between the hull and the propeller (see table) could pass currents up to 20a high which, in turn, may cause erosion of the bearing metal both on the shaft and the propeller. This phenomenon has been recently controlled by contact brush devices to short-circuit the shafting to the hull. This would eliminate the effect of the hull-propeller source. The three-electrode system discussed above is now becoming a two-electrode system.

Equations for currents flowing in the systems are expressed as follows

$$\begin{cases} i_2(R_{a.h}+R_{a.pr}+R_{h.pr})-i_3R_{a.h} = 0; \\ iR_{a.h}+i_3(R_{a.h}+R_h) = E_{c.p}. \end{cases}$$

By solving these equations we will obtain

the current between the anode and the hull

$$I_{a.h} = i_3-i_2 = \frac{E_{c.p}(R_{a.pr}+R_{h.pr})}{\Sigma R}; \tag{10}$$

the current between the anode and the propeller

$$I_{a.pr} = i_2 = \frac{E_{c.p}R_{a.h}}{\Sigma R} \tag{11}$$

where

$$\Sigma R = (R_{a.h}+R_h)(R_{a.h}+R_{a.pr}+R_{h.pr})-R_{a.h}^2.$$

Dividing equation (10) by (11), we will obtain the current short-circuited to the propeller

$$I_{a.h} = I_{a.pr}\frac{R_{a.pr}+R_{h.pr}}{R_{a.h}},$$

i.e. when $R_{a.h}>R_{a.pr}+R_{h.pr}$, most of the current will flow to the propeller. When $R_{a.h}=R_{a.pr}+R_{h.pr}$, the current $I_{a.pr}=I_{a.h}$.

The expressions obtained in this study indicate that the equality between the contact corrosion current and the protection current may be assumed as the approximate condition for protection against corrosion. Hence, in order to eliminate the propeller-hull voltaic couple and effect propeller protection against corrosion, it would be necessary to install contact-brush devices.

Example: Calculate the current of the hull-propeller couple on the ALATYR'LES motor ship.

1. The propeller leakage resistance

$$R_{le} = \frac{1}{\gamma r_0} \cdot \frac{K(k)}{K(k')} = 0{,}0077 \text{ ohm};$$

$$r_0 = 2{,}3 \text{ m}; \quad \gamma = 5 \text{ 1/ohm.m}; \quad h_0 = 2{,}5 \text{ m}$$

$$k = \frac{h_0 - r_0}{h_0 + r_0} = 0{,}0[illegible]; \quad k^2 = 0{,}0017; \quad k'^2 = 1 - k^2 = 0{,}9983.$$

From the elliptic integral tables [2] we will determine

K(k) = 1.57; K(k') = 3.69.

2. The hull polarization resistance

$R_h = 0.3/S_{pr} = 0.3/16.6 = 0.018$ ohm.

3. The internal resistance of a single bearing

$$\frac{1}{R} = [illegible] = 2{,}94 \frac{1}{\text{ohm}};$$

4. The resistance of all bearings (8 journal-type and 1 stern-type)

$$\sum_{i=1}^{9} [illegible] \frac{1}{\text{ohm}}; \quad R_{\Sigma} = \frac{1}{23{,}5} = 0{,}0425 \text{ ohm}.$$

4. The total resistance

$R_{tot} = 0.0077+0.018+0.0425 = 0.0682$ ohm.

5. The shafting current

$I_{h.pr} = U_h - U_{pr}/R_{tot} = 5.9a.$

Based on the measurements, the shafting current is 6.2a while the internal resistance

$R_{in} = tg\alpha = U/I = 0.230/6.2 = 0.0371$ ohm.

As may be seen, the calculated results are in fairly good agreement with the measurements.

REFERENCES

1. GUZEYEV, V.T. Determination of the Electrical Parameters of the Propeller-Shaft-Hull System and Their Practical Application. TRUDY TsNIIMFa (Transactions of the Central Scientific Research Institute of the Maritime Fleet), No. 99. Leningrad. "TRANSPORT" Publishing House,]968.

2. YANKE, E. and EMDE, F. TABLITSY FUNKTSIY S FORMULAMI I KRIVYMI (Tables of Functions With Formulas and Curves). MOSCOW, "GOSTEKHIZDAT" Publishing House,]948.

METHODS OF ACCELERATED CORROSION TESTING OF ORGANOSILICON COATINGS

[By M. Ya. Rozenblyum and L. A. Suprun. In "Tekhnicheskaya ekspluatatsiya morskogo flota. Teplokhimicheskiye issledovaniya. Bor'ba s korroziyey i obrastaniyem" (Technical Operations of the Maritime Fleet. Thermochemical Studies. Control of Corrosion and Fouling). Transaction of the Central Scientific Research Institute of the Maritime Fleet. No. 160, 1972. "Transport" Publishing House, Leningrad, pp. 89-93 Russian]

The capacitance-resistance method has been employed in many cases [13] to determine the protective properties of paint-and-varnish coatings; the procedure permits nondestructive quantitative evaluation of the coating. It has been known that the capacitance of the coating increases while its resistance decreases in the process of testing and destruction. An appropriate electric measuring circuit must be used for the system under study, otherwise the direct measurements would have to be recalculated to obtain true capacitance-resistance characteristics [2-3].

In the beginning of the test, when the coating is fairly continuous, the system being measured consists of a capacitance and a resistance connected in parallel (parallel connection). As the coating begins to fail, it develops continuous pores where the measured cell becomes a series-connected capacitance-resistance system. The capacitance-resistance connection diagram is determined from the frequency curve [3].

In these experiments involving the study of organosilicon coatings by the capacitance-resistance method using an R568 a-c bridge with a series connected capacitance and resistance at 1000-Hz frequencies and 30-mv operating voltages was initially found to increase to its maximum and then drop. This growth rate of the resistance for an either constant or increasing capacitance is probably related to the transition from a parallel capacitance-resistance connection diagram of the coating to a series-connected circuit. It is likely that only when the coating's resistance reaches its maximum, then it becomes a series-connected circuit in which the measured resistance represents the electrolyte's resistance in the pores of the coating. After the maximum is reached and the resistance decreases, the coating exhibits visible traces of corrosion. Thus, the time interval required for reaching maximum resistance characterizes the specific type of coating and may, therefore, be used as its

stability criterion. If, however, one should calculate the true resistance on the initial section of the curve with the capacitance and resistance connected in parallel, then the resistance-versus-time curve would smoothly descend with the typical signs of the onset of coating failure.

It has been known that tests can be accelerated by the use of more aggressive environments, higher temperatures, increased aeration, reduced coating thicknesses, etc. Unlike other techniques, reduced coating thicknesses accelerate coating failure without affecting the kinetics of the electrochemical process. The accelerated tests which will be described below were, therefore, conducted on thin film. The organosilicon test varnish coatings included K44, K47, and K54 grades; MgO, ZnO, Al_2O_3, TiO_2, Cr_2O_3, and Fe_2O_3 pigments and fillers. These test materials were applied by pouring on the surface of St.3 steel plates measuring 150x100x15 mm. Prior to painting, the metal surfaces were preconditioned by mechanical cleaning and degreasing with toluene. After application, the coatings were dried at 200°C for 2 hours so that the final coating thickness was 15μ. Glass cylinders, 35 mm in diameter and 50 mm high were filled with a 3% NaCl solution, to imitate sea water, were cemented to the painted plates. The test data on the corrosion resistance of the organosilicon varnishes are given in Figure 1. Based on the data obtained, K54 varnish was selected for further testing and used as a basis for compositions containing 5% of the said oxides (by volume); each composition contained only one type of pigment or filler.

Figure 2 shows test data on coatings containing ZnO, Cr_2O_3, and Fe_2O_3. Compositions with MgO, Al_2O_3 have not been cited in this figure since their protective properties were much lower than those of K54. The curves in Figure 3 show compositions with ZnO and Cr_2O_3 to have the higher resistance (35 and 30 days, respectively). The results shown by the composition with Fe_2O_3 were inferior to those with the first two oxides.

The corrosion resistance study of compositions containing ZnO and Cr_2O_3 in amounts ranging from 0 to 30%

THIS
PAGE
IS
MISSING
IN
ORIGINAL
DOCUMENT

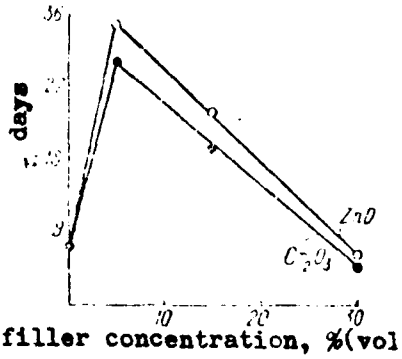

Figure 3. Effect of Filler Content on the Corrosion Resistance of the Coating

(by volume) shows 5% (by volume) to be the optimum filler content in the K54 varnish (Fig. 3). The accelerated test data have been summarized in a table. For comparison, the table provides also long-term test data on the same coating in thicknesses of about 100μ described in an earlier study [4]. As may be seen from the table, the first traces of corrosion appeared only after maximum resistance has been reached, while the difference between the time of appearance of initial corrosion traces and the test durations, corresponding to maximum resistance (coating stability) increases with the coating's thickness and its stability. The stability value obtained with the accelerated procedure correlates well with those of long-term tests. The resistance of organosilicon coatings of about 100μ in thickness is 45-52 times higher than those of 15μ. The conversion factor obtained permits calculation of coatings containing Cr_2O_3 and ZnO whose long-terms are yet to be completed.

Conclusions

1. The study of organosilicon coatings in a 3% NaCl solution by the capacitance-resistance method has shown that the measured resistance rises (in the beginning of testing) to its maximum with a slight increase in capacitance after which it begins to drop while the capacitance rapidly rises.

Results of Long-Term and Accelerated Corrosion Tests of Organosilicon Coatings

Coating	Test duration corresponding to maximum resistance τ_1, days	Time before appearance of initial corrosion traces, t_1, days	Test duration corresponding to maximum resistance, τ_2, days	Time before appearance of initial corrosion traces, t_2, days	Conversion factor τ_1/τ_2
	For coating thickness of 100μ		For coating thickness of 15μ		
K54	300	330	6	7	50
K47	210	240	4	5	52
K44	90	107	2	3	45
K54 + Cr_2O_3	Over 1380	-	30	40	-
K54 + ZnO	Over 1380	-	35	58	-
K54 + Fe_2O_3	450	480	10	14	45
K54 + Al_2O_3	-	-	1	1	-
K54 + TiO_2	-	-	1	1	-
K54 + MgO	-	-	5	7	-

2. The maximum resistance a characteristic and specific value for the coating under study; the traces of coating corrosion appear shortly after the maximum resistance has been reached.

3. The results of accelerated corrosion tests on organosilicon coatings correlate well with the data of long-term laboratory tests which indicates the feasible application of accelerated testing procedures for selecting organosilicon coatings.

ЛИТЕРАТУРА

1. [illegible] Н. Л., Жигалова К. А. Ускоренные методы [illegible] М., «Металлургия», 1966.

2. [illegible] Бурляченко В. Н., Жигалова К. А. О [illegible] лакокрасочных покрытий [illegible] «Лакокрасочные материалы и их применение», 1966, № [illegible]

3. [illegible] Бурляченко В. Н., Жигалова К. А. Результаты [illegible] свойств лакокрасочных покрытий [illegible] «Лакокрасочные материалы и их применение», 1966, № [illegible]

4. [illegible] М. Я., Орлов Н. Ф., Супрун Л. А. Исследование [illegible] кремнийорганических [illegible] Труды [illegible], вып. [illegible], 1971